ACS Catalysis

pubs.acs.org/acscatalysis
Research Article

Synthesis of 1*H*-Isoindole-Containing Scaffolds Enabled by a Nitrile Trifunctionalization

Àlex Díaz-Jiménez, Roger Monreal-Corona, Miquel Solà, Albert Poater,* Anna Roglans, and Anna Pla-Quintana*

Cite This: *ACS Catal.* 2024, 14, 7381−7388
Read Online

ACCESS | Metrics & More | Article Recommendations | Supporting Information

ABSTRACT: Nitrogen ring structures are widely found in biologically active compounds and natural products, making their construction an important area of focus in modern organic synthesis. In this work, the synthesis of products containing the 1*H*-isoindole motif has been successfully accomplished through a rhodium-catalyzed cascade, resulting in a significant increase in molecular complexity. This reaction, which encompasses the trifunctionalization of a nitrile moiety, is triggered by the formation of a nitrile ylide with extended conjugation by reaction of a rhodium vinylcarbene with a nitrile. The mechanism has been investigated by means of density functional theory calculations and supported through experimental data, enabling us to elucidate the precise steps that explain the rare nitrile trifunctionalization. A crucial step in this trifunctionalization is the attack of the second vinylcarbene to the azepine ring formed upon 1,7-electrocyclization of the nitrile ylide with extended conjugation.

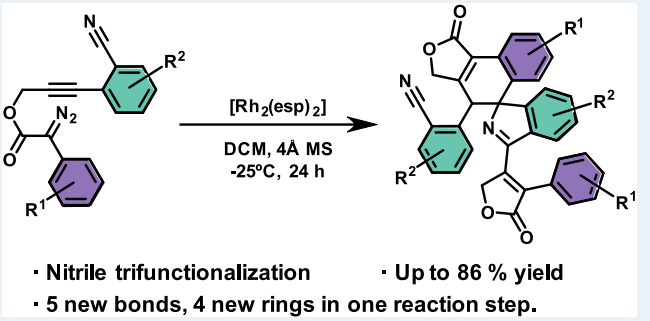

KEYWORDS: *cyclization reaction, fused 1H-isoindole, homogeneous rhodium catalysis, vinylcarbene, diazo compound*

INTRODUCTION

The construction of intricate ring structures containing nitrogen stands as a key focus in contemporary organic synthesis given their prevalence in biologically active compounds and natural products. Significant efforts have been directed toward creating reactions that tackle this goal in a rapid and efficient manner, with cascade reactions leveraging versatile reaction intermediates proving to be advantageous alternatives.[1]

Nitrile ylides are intriguing chemical compounds that play a crucial role as powerful intermediates in organic chemistry.[2] They are among the most reactive dipoles known,[3] capable of participating in 1,3-dipolar cycloadditions with CC, CN, CO, CS, NN, and NO multiple bonds, leading to the formation of various *N*-heterocyclic compounds. In addition to their intermolecular reaction pathways, nitrile ylides conveniently functionalized with multiple bonds readily give rise to heterocyclic molecules through 1,5-electrocyclization (Scheme 1A, left). Various methods exist for the preparation of nitrile ylides, and the direct reaction of a nitrile with an electrophilic carbene is particularly appealing. This approach offers a straighforward access to conjugated nitrile ylides, facilitating an easy entry to oxazoles,[4] pyrroles,[5] and imidazoles[6] through 1,5-electrocyclization.

If the conjugation is further extended, 1,7-electrocyclization can also occur (Scheme 1A, right), and a 1,5-H shift constitutes an insufficiently explored but very efficient way to access benzoazepine scaffolds. Seminal work was described by Padwa *et al.*[7] back in 1975 by generation of nitrile ylides *via* photochemical ring opening of azirine rings (Scheme 1B (i)) and was also explored by Sharp *et al.*[8] (Scheme 1B (ii)) although the process competed with a ring contraction. To the best of our knowledge, only one example of 1,7-electrocyclization involving a nitrile ylide generated by the reaction of a nitrile with a diazo compound has been described. Krasavin *et al.*[9] reported the rhodium-catalyzed reaction of a styryl diazo compound with a nitrile, generating a nitrile ylide with extended conjugation. Following 1,7-electrocyclization and a subsequent 1,5-H shift, the reaction resulted in the formation of tricyclic 2-benzazepines (Scheme 1B (iii)). A related transformation was reported in 2022 by Hashmi *et al.*[10] Phenanthridines were synthesized by reacting a vinylcarbene, generated through gold-catalyzed diazo-yne cyclization, with a nitrile. However, the cyclization did not involve the vinyl group of the *in situ* generated vinylcarbene; instead, the nucleophilic attack of a pendant aryl ring led to the formation of a 6-membered ring.

Received: February 9, 2024
Revised: April 11, 2024
Accepted: April 11, 2024
Published: April 26, 2024

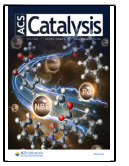

Scheme 1. (A) Reactivity Modes of Conjugated Nitrile Ylides, (B) State of the Art on 1,7-Electrocyclization Reactions, and (C) Our Preliminary Work on 1,7-Electrocyclization on a CAM Generated Nitrile Ylide[a]

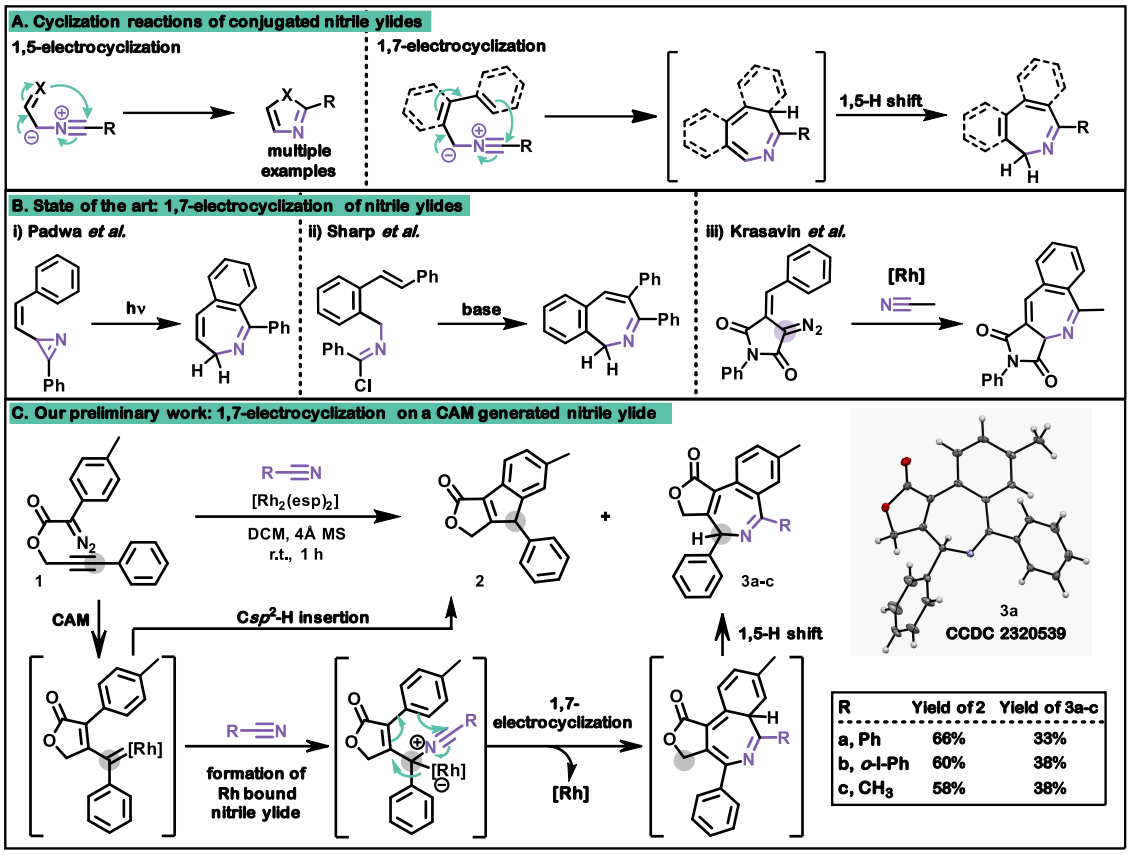

[a]esp = α,α,α′,α′-tetramethyl-1,3-benzenedipropionic acid, DCM = dichloromethane, MS = molecular sieves.

Carbene-alkyne metathesis (CAM) stands out as a potent transformation for the *in situ* generation of vinyl metal carbene intermediates,[11] particularly providing access to donor−donor carbenes that are dangerous to obtain directly from diazo compounds and whose reactivity is less explored.[12] In the course of our project aimed at the development of molecular complexity through the reaction of *in situ* generated vinyl metal carbenes,[13] we decided to explore whether a simple propargyl diazoacetate model was amenable to a CAM/nitrile ylide formation/1,7-electrocyclization reaction (Scheme 1C). Numerous challenges were faced, including difficulties in controlling the cascade order of the events and favoring the intermolecular reaction with the nitrile. Nonetheless, treatment of propargyl diazoacetate **1** with various nitriles under $[Rh_2(esp)_2]$ catalysis yielded two products. On one hand, the *in situ* generated donor−donor rhodium vinylcarbene inserted in the C(sp^2)−H bond leading to **2**, as already reported by Padwa *et al.*[14] and Doyle *et al.*[15] On the other hand, a benzoazepine derivative **3** was forged resulting from the anticipated cascade reaction.[16] In various reactions, product **3** was consistently the minor product, regardless of the amount of nitrile used.

RESULTS AND DISCUSSION

In our pursuit of developing a process with increased molecular complexity, we conceived the idea of synthesizing a propargyl diazoacetate conveniently functionalized with a nitrile group in a position where the formation of the nitrile ylide was not favored intramolecularly. Our goal of this work was to promote intermolecular reactions to enable a more prolonged cascade. Thus, we synthesized propargyl diazoacetate **4a** and investigated its reactivity. Following some optimization, in which lowering the temperature proved to be pivotal in controlling the reaction, we isolated a small quantity of a new product in a reaction catalyzed by $[Rh_2(esp)_2]$ (esp = α,α,α′,α′-tetramethyl-1,3-benzenedipropionic acid). Through spectroscopic characterization, particularly X-ray diffraction,[16] we confidently identified it as the azaspirocyclic compound **5a** (Scheme 2A). Of note, the formation of C(sp^2)−H inserted products analogous to **2** (Scheme 1C) was not observed. This product is a dimer constructed by forming up to five new bonds, including two C═C, one C═N, and two C−C bonds, in a process that generates four new cycles, all in a single reaction step. In addition to the remarkable increase in molecular complexity, this process has captivated interest from various other angles. The preparation of the 1*H*-isoindole core proves to be challenging[17] due to its inherent propensity to undergo isomerization, leading to the formation of aromatic isoindoles. Furthermore, it is a key motif found in AZD3839,[18] a potent and selective inhibitor of human BACE1 that reached clinical trials for Alzheimer's disease treatment as part of AstraZeneca's development. Spiroisoindoline-based molecules have also demonstrated utility as agrochemical pesticides[19] (Scheme 2B).

Since the formation of a product with 1*H*-isoindole core holds interest and relevance for its potential uses and furthermore does not align with what would typically be expected in a reaction between a nitrile and a metal

https://doi.org/10.1021/acscatal.4c00932
ACS Catal. 2024, 14, 7381−7388

Scheme 2. (A) Discovered Nitrile Ylide Dimerization Cascade, (B) Biologically Relevant Compounds Containing the 1*H*-Isoindole Motif, (C) General Reaction with Key Data on the Optimization Process, and (D) Reaction Scope[a]

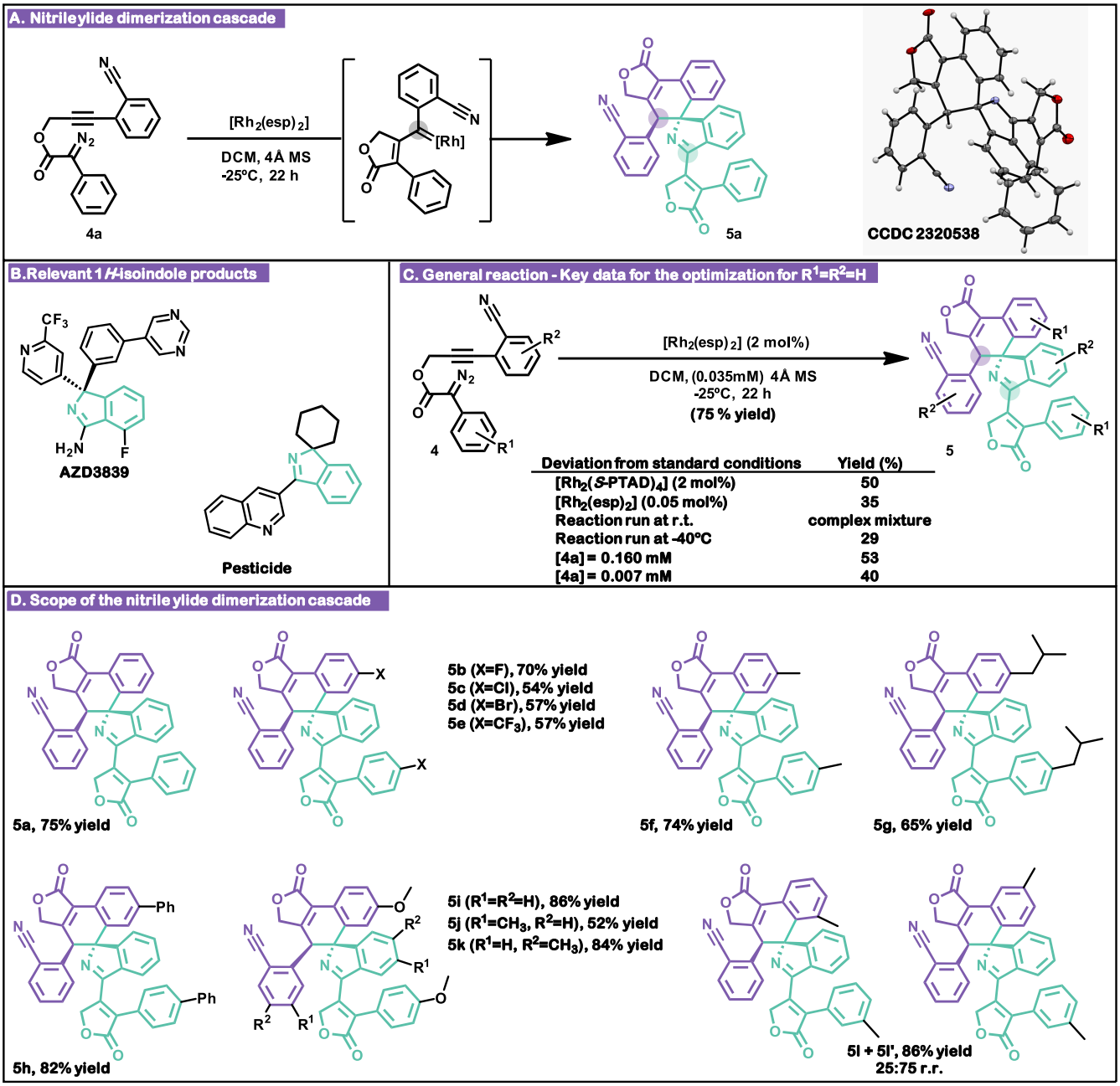

[a]Unless otherwise noted, reactions were performed at 0.035 M in dichloromethane (DCM) at −25 °C (with a stirring plate in the freezer) using 0.11 mmol of substrate and catalyst (2 mol %) under a N_2 atmosphere for 22 h

vinylcarbene, we decided to optimize the reaction conditions and we found that other complexes, such as $[Cu(MeCN)_4(PF_6)_2]$, $[Rh_2(OAc)_4]$ or $[Rh(COD)_2]BF_4$/(*R*)-BINAP, could not promote the reaction. The most critical parameters were found to be concentration and temperature, with the optimal results achieved at 0.035 M and −25 °C, yielding product **5a** in an excellent 75% yield (Scheme 2C, see the Supporting Information for the complete optimization). It is important to note that product **5a** has two stereocenters and was isolated as a single diastereomer in every case. With the optimized reaction conditions in hand, we evaluated the scope of the process (Scheme 2D). The catalytic reaction was successfully applied to substrates bearing different substituents in the *para* position of the 2-diazo-2-phenylacetate moiety. For example, derivatives containing electron-withdrawing halogen and CF_3 groups were efficiently converted into the desired products **5b**−**e**. While the introduction of a fluorine had no effect on the yield of **5b**, the introduction of chlorine, bromine, or trifluoromethyl reduced the overall yield to a range of 54−57%. The introduction of a methyl group in the same position resulted in the formation of **5f** with nearly the same yield as the unsubstituted substrate **5a**, and the introduction of an *iso*-butyl group slightly reduced the yield of **5g** to 65%. To examine the effect of an aromatic ring, a phenyl group was introduced in the *para* position in substrate **4h**, resulting in a reaction with an excellent yield. The effect of introducing a methoxy group with

https://doi.org/10.1021/acscatal.4c00932
ACS Catal. 2024, 14, 7381−7388

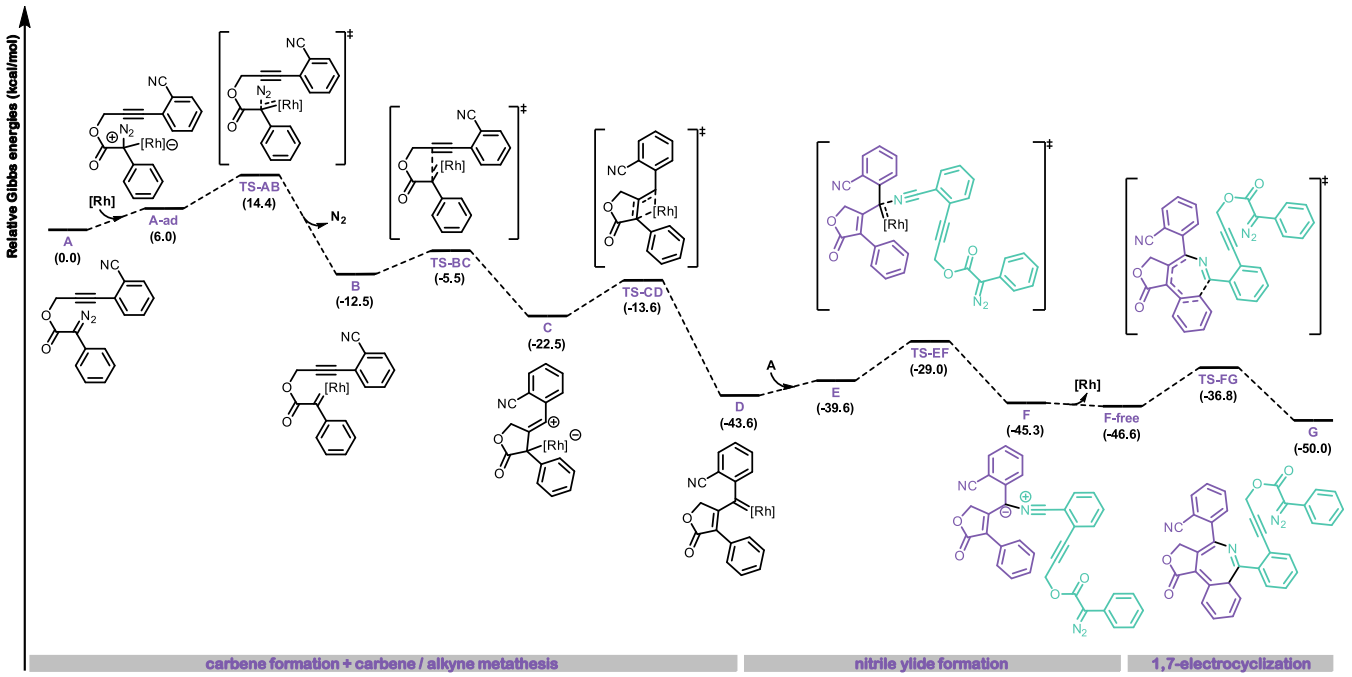

Figure 1. DFT computed first carbene formation and carbene-alkyne metathesis, nitrile ylide formation, and 1,7-electrocyclization of **4a**. Gibbs energies (298 K) relative to **4a** and $[Rh_2(OOCH)_4]$ are shown in kcal/mol ([Rh] = $[Rh_2(OOCH)_4]$).

increased electron-donating character provided **5i** with an excellent yield. In summary, the yield of the reaction increases with electron-donating groups. At this point, we also decided to analyze the effect of introducing substituents to the benzonitrile ring on the substrate already containing a methoxy group in the 2-diazo-2-phenylacetate moiety. The introduction of a methyl ring at the *para* position to the cyano moiety considerably reduced the yield (compare the results of **5i** to **5j**). Surprisingly, the introduction of a methyl in the *para* position to the alkyne in **4k** resulted in a reaction with excellent yield. Finally, a methyl group was introduced to the 2-diazo-2-phenylacetate moiety but in the *meta* position. Not unexpectedly, the reaction was efficient but provided a mixture of regioisomers in a 25:75 relative ratio. Due to the challenges in assigning the two regioisomers **5l** and **5l′** solely through NMR spectroscopy, density functional theory (DFT) calculations were employed to verify that the major isomer was the less sterically hindered one, wherein the methyl group remains in *para* to the 1*H*-isoindole ring (refer to Section S12 for details).

In an effort to comprehend the mechanism underlying the discovered transformation, a series of DFT calculations at the B3LYP-D3/6−311+G**~LANL2DZ-SMD(DCM)//B3LYP-D3/6−31+G*~LANL2DZ level of theory were performed using the Gaussian16 software package (see Supporting Information for further details).[20] We initiated our investigation by examining the pathway leading to the formation of the rhodium vinylcarbene species **D**, originating from the carbene-alkyne metathesis and subsequent intermolecular nitrile attack on the rhodium vinylcarbene (Figure 1). Given the size and complexity of the system involving two substrate molecules and the associated computational cost, we chose to employ $[Rh_2(OOCH)_4]$ as a truncated model[11,21] of the catalytic system experimentally used in our experiments. The reaction starts by coordination of the rhodium complex to the carbon linked to the diazo moiety in a mildly endergonic step (6.0 kcal/mol). This step is followed by the extrusion of nitrogen through transition state **TS-AB**, with an overall energy barrier of 14.4 kcal/mol with respect to reactants **A** and $[Rh_2(OOCH)_4]$, leading to rhodium carbene **B** (−12.5 kcal/mol). Following this, a nucleophilic attack of the alkyne onto the carbenic carbon induces a 5-exo-dig cyclization, yielding zwitterionic vinyl cationic species **C** in an exergonic step (10.0 kcal/mol) with an energy barrier of 7.0 kcal/mol. The reaction progresses further with the nucleophilic attack of the negatively charged rhodium atom on the carbocation, directly giving rise to the rhodium η^1-vinylcarbene **D**, surpassing a reaction barrier of 8.9 kcal/mol. At this point, a second molecule of substrate **A** comes into play. Upon coordination, the carbenic carbon of the η^1-vinylcarbene **D** unit accepts an electron pair from the nitrile moiety of **A**, yielding rhodium-bound nitrile ylide **F** in a mildly exergonic process (1.7 kcal/mol) that surpasses an energy barrier of 14.6 kcal/mol. The process continues with the formation of the rhodium unbound nitrile ylide **F-free**, releasing 1.3 kcal/mol of energy. Overall, the formation of nitrile ylide **F-free** is very exergonic (46.6 kcal/mol). Depending on the substituents, nitrile ylides can be categorized as the propargyl type or the allenyl type. The bending on the N−C−C(Ph) unit, with an angle of 167.1°, indicates that **F-free** is best described as a 2-azonia-allenyl anion, as already observed for vinyl nitrile ylides by Fabian *et al.*[22] This bending facilitates 1,7-electrocyclization through **TS-FG**, which has an activation energy of 9.8 kcal/mol. This process is only mildly exergonic (3.4 kcal/mol), most likely due to the loss of aromaticity of one of the six-membered rings in intermediate **G**.

Upon formation of intermediate species **G**, two different possibilities were considered: the formation of a rhodium carbene by the reaction of the catalyst with the diazo unit or a 1,5-hydride shift to forge a benzoazepine core in a process analogous to what was observed through the reaction with nitrile derivatives (Scheme 1C) (the Gibbs energy profile

https://doi.org/10.1021/acscatal.4c00932
ACS Catal. 2024, 14, 7381−7388

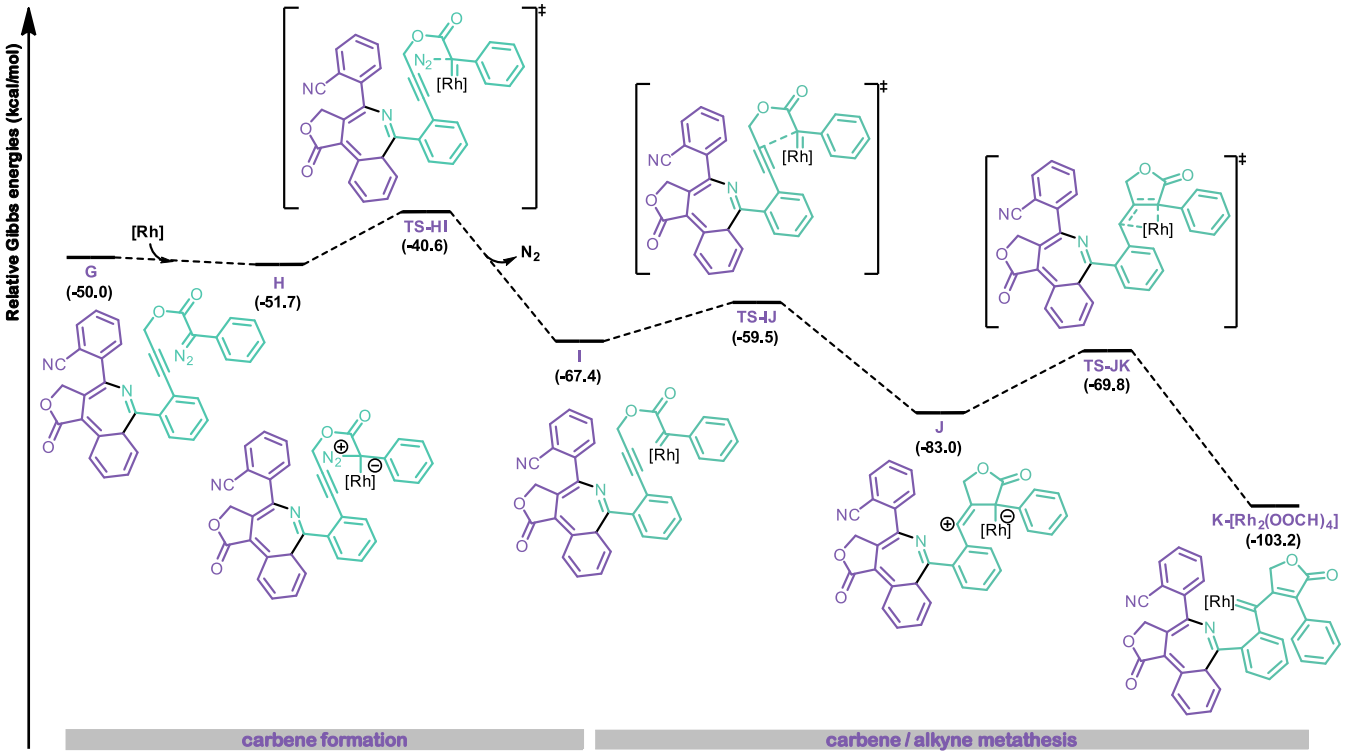

Figure 2. DFT computed second carbene formation and carbene-alkyne metathesis. Gibbs energies (298 K) relative to **4a** and $[Rh_2(OOCH)_4]$ are shown in kcal/mol ([Rh] = $[Rh_2(OOCH)_4]$).

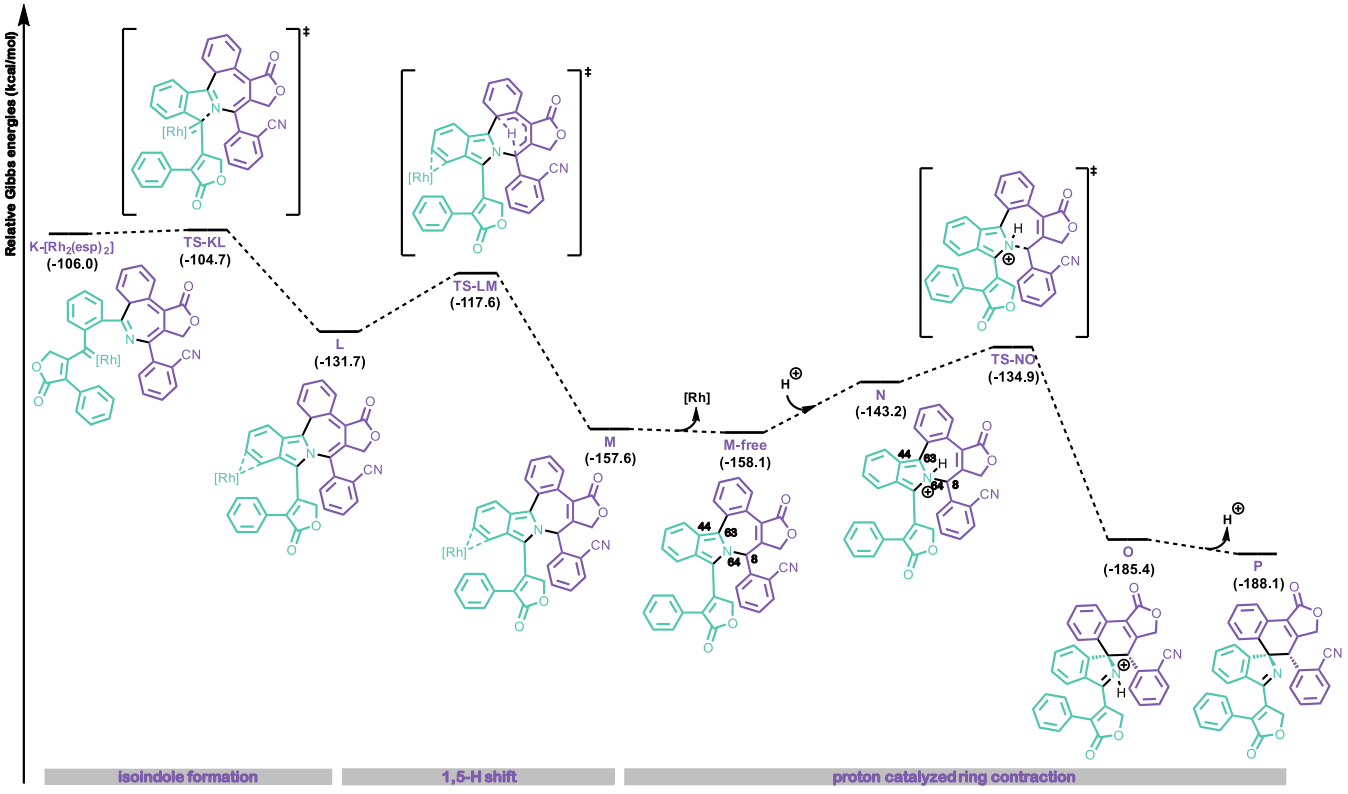

Figure 3. DFT computed electrocyclization, isoindole formation, 1,5-H shift, and proton-catalyzed ring contraction for the formation of **5a**. Gibbs energies (298 K) relative to **4a** and $[Rh_2(esp)_2]$ are shown in kcal/mol ([Rh] = $[Rh_2(esp)_2]$).

comparing both pathways is shown in Figure S1). The latter was disregarded due to its higher kinetic cost. Thus, the reaction evolves via carbene formation and CAM (Figure 2). Indeed, species **G** coordinates with the Rh catalyst to form adduct **H**, and then proceeds through the nitrogen extrusion step **TS-HI** with a relative activation energy of 11.1 kcal/mol.

https://doi.org/10.1021/acscatal.4c00932
ACS Catal. 2024, 14, 7381−7388

From the metal carbene species **I**, a 5-exo-dig cyclization surpassing a reaction barrier of 7.9 kcal/mol yields the zwitterionic vinyl cationic species **J** and subsequent nucleophilic attack of the negatively charged rhodium atom on the carbocation gives rise to the rhodium η^1-vinylcarbene **K**-[$Rh_2(OOCH)_4$], surpassing a reaction barrier of 13.2 kcal/mol, in a process analogous to the one observed in the first CAM.

We then decided to run the calculations from this point with the actual [$Rh_2(esp)_2$] catalyst (Figure 3) due to the considerable geometric differences that conditioned the outcome of the reaction. Substitution of formate by esp ligands results in a difference of 2.8 kcal/mol in the relative energies of **K**-[$Rh_2(OOCH)_4$] and **K**-[$Rh_2(esp)_2$]. From **K**-[$Rh_2(esp)_2$], we analyzed two alternative reaction pathways (see Figure S2). At first, **K**-[$Rh_2(esp)_2$] evolves through a 1,5-H shift, surpassing an energy barrier of 17.7 kcal/mol to forge the benzoazepine core. Second, there is a nucleophilic attack of the azepine N atom to the carbenic carbon, yielding the isoindole derivative **L** through a kinetically very favorable reaction (1.3 kcal/mol reaction barrier, Figure 3). From intermediate **L**, to which the rhodium is not fully coordinated but interacts with the isoindole ring, a 1,5-H shift takes place through **TS-LM**, recovering the aromaticity of the six-membered ring fused to the azepine, with an energy barrier of 14.1 kcal/mol and releasing 25.9 kcal/mol, in part due to the aromatization of this six-membered ring. At this point, the rhodium leaves the system closing the rhodium-catalyzed cycle. However, a ring contraction is still needed to explain the formation of the final product. After exploring various possibilities (see Figure S3), we found that a proton catalyzes this final ring contraction.[23,24] Protonation of the isoindole nitrogen changes the geometry around the nitrogen from roughly planar (C8−N64−C63−C44 dihedral angle 170.8° (refer to Figure 3 for atom labeling)) to roughly tetrahedral (dihedral angle 116.6°). This geometry change enables ring contraction, surpassing that of **TS-NO** with an activation energy of 23.2 kcal/mol. This exergonic step (27.3 kcal/mol) leads to **O**, which upon deprotonation results in the formation of isolated product **P**. The formation of the other diastereoisomer was also computationally evaluated by analyzing the protonation on the other side of the nitrogen. However, the reaction path was found to be unproductive (see Figure S4).

Even though the reaction is conducted under anhydrous conditions, we postulate that this last part of the transformation occurs upon opening the reaction flask or due to the treatment of the crude reaction mixture with silica gel, as evidenced by a noticeable color change. Unfortunately, all efforts to experimentally detect the intermediate **M-free** have proven to be unsuccessful. Conversely, given that the formation of compound **5** involves the migration of a hydrogen atom from the phenylacetic ring in **4**, we prepared the corresponding C_6D_5 derivative **4a-d$_5$** to assess the fate of this H(D) (Scheme 3). Product **5a-d$_{10}$** was obtained, with the deuterium originating from the C−D cleavage located exclusively in the position anticipated for a 1,5-H shift consistent with the proposed mechanism and with no scrambling into other positions.

In summary, the rhodium-catalyzed reaction (**A** to **M**) has an overall Gibbs reaction energy of −157.6 kcal/mol through a highly extended cascade process. The energetic span between the turnover frequency (TOF) determining intermediate

Scheme 3. Deuterium Labeling Experiment

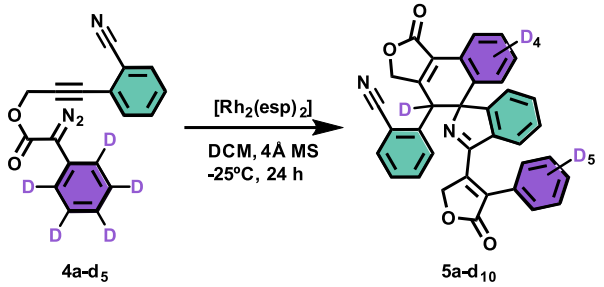

(TDI, **D**) and the TOF determining transition state (TDTS, **TS-EF**) is 14.6 kcal/mol.[25] However, the energetic span in this nitrile ylide formation step is almost isoenergetic to that in the carbene formation step (span from TDI **A** to TDTS **TS-AB** is 14.4 kcal/mol) and the 1,5-H shift (span from TDI **H** to TDTS **TS-HI** is 14.1 kcal/mol). The proton-catalyzed ring contraction is a separate process that we postulate occurs during the reaction workup and releases 2.7 kcal/mol.

An alternative pathway, involving the reaction of two units of vinylcarbene intermediate **D**, has also been evaluated (see Figure S5). This alternative pathway has an almost isoenergetic span between the TOF determining intermediate (TDI) and the TOF determining transition state (TDTS) and is not competitive with the limiting or selective steps. Although the two pathways can coexist, given the low probability of two carbenes lasting enough to react with one another, we believe that the pathway shown in Figures 1−3 is more favorable under the reaction conditions used. It is important to note that the transformation globally encompasses a trifunctionalization of the nitrile moiety, which is a quite exceptional transformation, involving the generation of two new bonds to the C(sp) of the nitrile, triggering the formation of the 1*H*-isoindole moiety. Key to this trifunctionalization is the attack of the azepine N atom on a rhodium vinylcarbene. This new method adds to the portfolio of selected transformations that control the reactions of highly active chemical species, enabling the straightforward synthesis of valuable polycyclic compounds.[26]

CONCLUSIONS

In conclusion, we have presented a novel cascade process leading to a significant enhancement in molecular complexity for the diastereoselective synthesis of products containing the 1*H*-isoindole motif. An isotope labeling experiment and an in-depth computational study have elucidated the reaction pathway, encompassing both a rhodium-catalyzed and a proton-catalyzed steps. The current reaction leverages the specific reactivity of *in situ* generated donor−donor rhodium carbenes, taking advantage of the versatility of these intermediates, which in this intricate cascade selectively react at different points in the catalytic cycle.

ASSOCIATED CONTENT

Supporting Information

The Supporting Information is available free of charge at https://pubs.acs.org/doi/10.1021/acscatal.4c00932.

Experimental procedures, compound characterization data including NMR spectra for all compounds, and crystallographic data; alternative reaction pathways (PDF)

https://doi.org/10.1021/acscatal.4c00932
ACS Catal. 2024, 14, 7381−7388

Crystallographic data (CIF)
Crystallographic data (CIF)
XYZ Cartesian coordinates (XYZ)

AUTHOR INFORMATION

Corresponding Authors

Albert Poater − *Institut de Química Computacional i Catàlisi (IQCC) and Departament de Química, Facultat de Ciències, Universitat de Girona (UdG), Girona, Catalunya 17003, Spain;* orcid.org/0000-0002-8997-2599; Email: albert.poater@udg.edu

Anna Pla-Quintana − *Institut de Química Computacional i Catàlisi (IQCC) and Departament de Química, Facultat de Ciències, Universitat de Girona (UdG), Girona, Catalunya 17003, Spain;* orcid.org/0000-0003-2545-9048; Email: anna.plaq@udg.edu

Authors

Àlex Díaz-Jiménez − *Institut de Química Computacional i Catàlisi (IQCC) and Departament de Química, Facultat de Ciències, Universitat de Girona (UdG), Girona, Catalunya 17003, Spain;* orcid.org/0000-0003-1241-8263

Roger Monreal-Corona − *Institut de Química Computacional i Catàlisi (IQCC) and Departament de Química, Facultat de Ciències, Universitat de Girona (UdG), Girona, Catalunya 17003, Spain;* orcid.org/0000-0003-3071-9887

Miquel Solà − *Institut de Química Computacional i Catàlisi (IQCC) and Departament de Química, Facultat de Ciències, Universitat de Girona (UdG), Girona, Catalunya 17003, Spain;* orcid.org/0000-0002-1917-7450

Anna Roglans − *Institut de Química Computacional i Catàlisi (IQCC) and Departament de Química, Facultat de Ciències, Universitat de Girona (UdG), Girona, Catalunya 17003, Spain;* orcid.org/0000-0002-7943-5706

Complete contact information is available at: https://pubs.acs.org/10.1021/acscatal.4c00932

Author Contributions

The manuscript was written through contributions of all authors. All authors have given approval to the final version of the manuscript.

Notes

The authors declare no competing financial interest.

ACKNOWLEDGMENTS

We are grateful for financial support from the Ministerio de Ciencia e Innovación (PID2021-127423NB-I00 and PID2020-113711GB-I00 MCIN/AEI/10.13039/501100011033 projects) and the Generalitat de Catalunya (Project 2021-SGR-623). We thank the Spanish Ministerio de Universidades for the predoctoral fellowship FPU18/02912 to A.D.-J. and FPU20/00707 to R.M.-C. A.P.Q. and A.P. are Serra Húnter Fellows, and A.P. thanks ICREA Academia Prize 2019.

REFERENCES

(1) For selected book chapter and reviews, see: (a) Faisca Phillips, A. M. M. M. Asymmetric Organocatalytic Cascade Reactions for the Synthesis of Nitrogen Heterocycles. In *More Synthetic Approaches to Nonaromatic Nitrogen Heterocycles*; Faisca Phillips, A. M. M. M., Ed.; John Wiley & Sons: Hoboken, 2022; Vol. *1*, pp 101−161. (b) Zhang, B.; Studer, A. Recent Advances in the Synthesis of Nitrogen Heterocycles via Radical Cascade Reactions using Isonitriles as Radical Acceptors. *Chem. Soc. Rev.* **2015**, *44* (11), 3505−3521. For selected recent examples, see: (c) Song, L.; Tian, X.; Farshadfar, K.; Shiri, F.; Rominger, F.; Ariafard, A.; Hashmi, A. S. K. An Unexpected Synthesis of Azepinone Derivatives through a Metal-Free Photochemical Cascade Reaction. *Nat. Commun.* **2023**, *14* (1), 831.

(2) Escolano, C.; Duque, M. D.; Vázquez, S. Nitrile Ylides: Generation, Properties and Synthetic Applications. *Curr. Org. Chem.* **2007**, *11* (9), 741−772.

(3) Huisgen, R.; Stangl, H.; Sturm, H. J.; Wagenhofer, H. 1,3-Dipolare Additionen mit Nitril-yliden. *Angew. Chem.* **1962**, *74*, 31−31.

(4) For reviews on Rh-catalyzed synthesis of oxazoles, see: (a) Bresciani, N.; Tomkinson, N. C. Transition Metal-Mediated Synthesis of Oxazoles. *Heteroat. Chem.* **2014**, *89* (11), 2479−2543. (b) Budeev, A.; Kantin, G.; Dar'in, D.; Krasavin, M. Diazocarbonyl and Related Compounds in the Synthesis of Azoles. *Molecules* **2021**, *26*, 2530. For selected examples of preparation of oxazoles with other metals, see: (c) He, W.; Li, C.; Zhang, L. An Efficient [2 + 2 + 1] Synthesis of 2,5-Disubstituted Oxazoles via Gold-Catalyzed Intermolecular Alkyne Oxidation. *J. Am. Chem. Soc.* **2011**, *133*, 8482−8485. (d) Su, H.; Bao, M.; Pei, C.; Hu, W.; Qiu, L.; Xu, X. Gold-Catalyzed Dual Annulation of Azide-Tethered Alkynes with Nitriles: Expeditious Synthesis of Oxazolo[4,5-c]quinolines. *Org. Chem. Front.* **2019**, *6*, 2404−2409. (e) Wang, Q.; Rudolph, M.; Rominger, F.; Hashmi, A. S. K. Gold-Catalyzed Intermolecular Oxidative Diyne Cyclizations via 1,6-Carbene Transfer. *Adv. Synth. Catal.* **2020**, *362*, 755−759. (f) Prashanth, S.; Adarsh, D. R.; Bantu, R.; Sridhar, B.; Reddy, B. V. S. Cu(II)-Catalyzed Synthesis of 2,4,5-Trisubstituted Oxazoles. *Tetrahedron Lett.* **2022**, *113*, 154252. For a photoinduced version, see: (g) Saha, A.; Sen, C.; Guin, S.; Das, C.; Maiti, D.; Sen, S.; Maiti, D. Photoinduced [3 + 2] Cycloaddition of Carbenes and Nitriles: A Versatile Approach to Oxazole Synthesis. *Angew. Chem., Int. Ed.* **2023**, *62*, No. e202308916.

(5) For selected examples of preparation of pyrroles with coinage metal catalysis, see: (a) Billedeau, R. J.; Klein, K. R.; Kaplan, D.; Lou, Y. A New Pyrrole Synthesis via Silver(I)-Catalyzed Cycloaddition of Vinylogous Diazoester and Nitrile. *Org. Lett.* **2013**, *15*, 1421−1423. (b) Lonzi, G.; López, L. A. Regioselective Synthesis of Functionalized Pyrroles via Gold(I)-Catalyzed [3 + 2] Cycloaddition of Stabilized Vinyl Diazo Derivatives and Nitriles. *Adv. Synth. Catal.* **2013**, *355*, 1948−1954.

(6) Xiao, Y.; Zhang, L. Synthesis of Bicyclic Imidazoles via [2 + 3] Cycloaddition between Nitriles and Regioselectively Generated α-Imino Gold Carbene Intermediates. *Org. Lett.* **2012**, *14*, 4662−4665.

(7) Padwa, A.; Smolanoff, J.; Tremper, A. Intramolecular Cycloaddition Reactions of Vinyl-Substituted 2H-Azirines. *J. Am. Chem. Soc.* **1975**, *97*, 4682−4691.

(8) Motion, K. R.; Robertson, I. R.; Sharp, J. T.; Walkinshaw, M. D. Reactions of Diene-Conjugated 1,3-Dipolar Intermediates: the Formation of Cyclopropa[c]isoquinolines from Benzonitrile o-Alkenylbenzyl Ylides and their Rearrangements to Benzazepines. *J. Chem. Soc., Perkin Trans.* **1992**, *1*, 1709−1719.

(9) Inyutina, A.; Dar'in, D.; Kantin, G.; Krasavin, M. Tricyclic 2-Benzazepines Obtained via an Unexpected Cyclization Involving Nitrilium Ylides. *Org. Biomol. Chem.* **2021**, *19*, 5068−5071.

(10) Zhang, C.; Chen, Q.; Wang, L.; Sun, Q.; Yang, Y.; Rudolph, M.; Rominger, F.; Hashmi, A. S. K. Practical and Modular Construction of Benzo[c]phenanthridine Compounds. *Sci. China Chem.* **2022**, *65*, 1338−1346.

(11) (a) For seminal works, see: Padwa, A.; Blacklock, T. J.; Loza, R. Silver-Promoted Isomerizations of Some Cyclopropene Derivatives. *J. Am. Chem. Soc.* **1981**, *103*, 2404−2405. (b) Padwa, A.; Xu, S. L. A New Phenol Synthesis from the Rhodium(I) Catalyzed Reaction of Cyclopropenes and Alkynes. *J. Am. Chem. Soc.* **1992**, *114* (14), 5881−5882. (c) Hoye, T. R.; Dinsmore, C. J. Rhodium(II) Acetate Catalyzed Alkyne Insertion Reactions of α-Diazo Ketones: Mechanistic Inferences. *J. Am. Chem. Soc.* **1991**, *113*, 4343−4345. For reviews, see: (d) Pei, C.; Zhang, C.; Qian, Y.; Xu, X. Catalytic Carbene/Alkyne Metathesis (CAM): a Versatile Strategy for Alkyne

Bifunctionalization. *Org. Biomol. Chem.* **2018**, *16*, 8677−8685. (e) Torres, Ò.; Pla-Quintana, A. The Rich Reactivity of Transition Metal Carbenes with Alkynes. *Tetrahedron Lett.* **2016**, *57*, 3881−3891. For selected recent advances, see: (f) Wang, X.; Zhou, Y.; Qiu, L.; Yao, R.; Zheng, Y.; Zhang, C.; Bao, X.; Xu, X. Enantioselective Carbene Cascade: An Effective Approach to Cyclopentadienes and Applications in Diels−Alder Reactions. *Adv. Synth. Catal.* **2016**, *358* (10), 1571−1576. (g) Dong, K.; Fan, X.; Pei, C.; Zheng, Y.; Chang, S.; Cai, J.; Qiu, L.; Yu, Z.-X.; Xu, X. Transient-Axial-Chirality Controlled Asymmetric Rhodium-Carbene C(sp^2)-H Functionalization for the Synthesis of Chiral Fluorenes. *Nat. Commun.* **2020**, *11*, 2363. (h) Bao, M.; Xie, X.; Hu, W.; Xu, X. Gold-Catalyzed Carbocyclization/C = N Bond Formation Cascade of Alkyne-Tethered Diazo Compounds with Benzo[c]isoxazoles for the Assembly of 4-Iminonaphthalenones and Indenes. *Adv. Synth. Catal.* **2021**, *363*, 4018−4023. (i) Zhang, C.; Hong, K.; Dong, S.; Liu, M.; Rudolph, M.; Dietl, M. C.; Yin, J.; Hashmi, A. S. K.; Xu, X. Generation and Utility of Cyclic Dienyl Gold Carbene Intermediates. *ACS Catal.* **2023**, *13*, 4646−4655.

(12) (a) Zhu, D.; Chen, L.; Fan, H.; Yao, Q.; Zhu, S. Recent Progress on Donor and Donor-Donor Carbenes. *Chem. Soc. Rev.* **2020**, *49*, 908−950. (b) Bergstrom, B. D.; Nickerson, L. A.; Shaw, J. T.; Souza, L. W. Transition Metal Catalyzed Insertion Reactions with Donor/Donor Carbenes. *Angew. Chem., Int. Ed.* **2021**, *60*, 6864−6878.

(13) (a) Torres, Ò.; Parella, T.; Solà, M.; Roglans, A.; Pla-Quintana, A. Enantioselective Rhodium(I) Donor Carbenoid-Mediated Cascade Triggered by a Base-Free Decomposition of Arylsulfonyl Hydrazones. *Chem. Eur. J.* **2015**, *21* (45), 16240−16245. (b) Torres, Ò.; Roglans, A.; Pla-Quintana, A. An Enantioselective Cascade Cyclopropanation Reaction Catalyzed by Rhodium(I): Asymmetric Synthesis of Vinylcyclopropanes. *Adv. Synth. Catal.* **2016**, *358*, 3512−3516. (c) Torres, Ò.; Solà, M.; Roglans, A.; Pla-Quintana, A. Unusual Reactivity of Rhodium Carbenes with Allenes: An Efficient Asymmetric Synthesis of Methylenetetrahydropyran Scaffolds. *Chem. Commun.* **2017**, *53*, 9922−9925. (d) Díaz-Jiménez, À.; Monreal-Corona, R.; Poater, A.; Álvarez, M.; Borrego, E.; Pérez, P. J.; Caballero, A.; Roglans, A.; Pla-Quintana, A. Intramolecular Interception of the Remote Position of Vinylcarbene Silver Complex Intermediates by C(sp^3)−H Bond Insertion. *Angew. Chem., Int. Ed.* **2023**, *135* (5), No. e202215163.

(14) Padwa, A.; Weingarten, M. D. Rhodium(II)-Catalyzed Carbocyclization Reaction of α-Diazo Carbonyls with Tethered Unsaturation. *J. Org. Chem.* **2000**, *65*, 3722−3732.

(15) Qiu, H.; Deng, Y.; Marichev, K. O.; Doyle, M. P. Diverse Pathways in Catalytic Reactions of Propargyl Aryldiazoacetates: Selectivity between Three Reaction Sites. *J. Org. Chem.* **2017**, *82*, 1584−1590.

(16) Deposition number 2320539 (for **3a** (R = Ph)) and 2320538 (for **5a**) contain the supplementary crystallographic data for this paper. These data are provided free of charge by the joint Cambridge Crystallographic Data Centre and Fachinformationszentrum Karlsruhe Access Structure service.

(17) For a review, see: (a) Weintraub, R. A.; Wang, X. Recent Developments in Isoindole Chemistry. *Synthesis* **2023**, *55*, 519−546. For selected recent examples, see: (b) Grosheva, D.; Cramer, N. Enantioselective Access to 1*H*-Isoindoles with Quaternary Stereogenic Centers by Palladium(0)-Catalyzed C−H Functionalization. *Angew. Chem., Int. Ed.* **2018**, *130* (41), 13832−13835. (c) Wang, J.; Li, L.; Chai, M.; Ding, S.; Li, J.; Shang, Y.; Zhao, H.; Li, D.; Zhu, Q. Enantioselective Construction of 1H-Isoindoles Containing Tri- and Difluoromethylated Quaternary Stereogenic Centers via Palladium-Catalyzed C-H bond Imidoylation. *ACS Catal.* **2021**, *11*, 12367−12374.

(18) Jeppsson, F.; Eketjäll, S.; Janson, J.; Karlström, S.; Gustavsson, S.; Olsson, L.-L.; Radesäter, A.-C.; Ploeger, B.; Cebers, G.; Kolmodin, K.; Swahn, B.-M.; von Berg, S.; Bveters, T.; Fälting, J. Discovery of AZD3839, a Potent and Selective BACE1 Inhibitor Clinical Candidate for the Treatment of Alzheimer Disease. *J. Biol. Chem.* **2012**, *287*, 41245−41257.

(19) Hiroyuki, I.; Kota, F. Sankyo Agro KK. 2008. JP 2,008,088,139 A.

(20) Frisch, M. J.; Trucks, G. W.; Schlegel, H. B.; Scuseria, G. E.; Robb, M. A.; Cheeseman, J. R.; Scalmani, G.; Barone, V.; Mennucci, B.; Petersson, G. A.; Nakatsuji, H.; Caricato, M.; Li, X.; Hratchian, H. P.; Izmaylov, A. F.; Bloino, J.; Zheng, G.; Sonnenberg, J. L.; Hada, M.; Ehara, M.; Toyota, K.; Fukuda, R.; Hasegawa, J.; Ishida, M.; Nakajima, T.; Honda, Y.; Kitao, O.; Nakai, H.; Vreven, T.; Montgomery, J. A.; Peralta, J. E.; Ogliaro, F.; Bearpark, M.; Heyd, J. J.; Brothers, E.; Kudin, K. N.; Staroverov, V. N.; Kobayashi, R.; Normand, J.; Raghavachari, K.; Rendell, A.; Burant, J. C.; Iyengar, S. S.; Tomasi, J.; Cossi, M.; Rega, N.; Millam, J. M.; Klene, M.; Knox, J. E.; Cross, J. B.; Bakken, V.; Adamo, C.; Jaramillo, J.; Gomperts, R.; Stratmann, R. E.; Yazyev, O.; Austin, A. J.; Cammi, R.; Pomelli, C.; Ochterski, J. W.; Martin, R. L.; Morokuma, K.; Zakrzewski, V. G.; Voth, G. A.; Salvador, P.; Dannenberg, J. J.; Dapprich, S.; Daniels, A. D.; Farkas, Ö.; Foresman, J. B.; Ortiz, J. V.; Cioslowski, J.; Fox, D. J. *Gaussian 16*; Gaussian Inc.: Wallingford, CT, 2016.

(21) For recent examples in which analogous truncations have been used, see: (a) Zhu, D.; Cao, T.; Chen, K.; Zhu, S. Rh_2(II)-Catalyzed Enantioselective Intramolecular Büchner Reaction and Aromatic Substitution of Donor-Donor Carbenes. *Chem. Sci.* **2022**, *13*, 1992−2000. (b) Hong, K.; Zhou, Y.; Yuan, H.; Zhang, Z.; Huang, J.; Dong, S.; Hu, W.; Yu, Z.-X.; Xu, X. Catalytic 4-exo-dig Carbocyclization for the Construction of Furan-Fused Cyclobutanones and Synthetic Applications. *Nat. Commun.* **2023**, *14*, 6378.

(22) Fabian, W. M. F.; Kappe, C. O.; Bakulev, V. A. Ab Initio and Density Functional Calculations on the Pericyclic vs Pseudopericyclic Mode of Conjugated Nitrile Ylide 1,5-Electrocyclizations. *J. Org. Chem.* **2000**, *65*, 47−53.

(23) The value of $\Delta G_{aq}(H^+)$ considered in DCM that has been used is 250.0 kcal/mol, considering that when the reaction flask is opened there would be the potential presence of water and the value would tend towards the value of 272.2 kcal/mol in pure water.

(24) Acuña-Parés, F.; Codolà, Z.; Costas, M.; Luis, J. M.; Lloret-Fillol, J. Unraveling the Mechanism of Water Oxidation Catalyzed by Nonheme Iron Complexes. *Chem. Eur. J.* **2014**, *20*, 5696−5707.

(25) (a) Kozuch, S.; Shaik, S. Kinetic-Quantum Chemical Model for Catalytic Cycles: the Haber−Bosch Process and the Effect of Reagent Concentration. *J. Phys. Chem. A* **2008**, *112*, 6032−6041. (b) Kozuch, S.; Shaik, S. How to Conceptualize Catalytic Cycles? The Energetic Span Model. *Acc. Chem. Res.* **2011**, *44*, 101−110.

(26) Harada, S. Development of Novel Methodology Using Diazo Compounds and Metal Catalysts. *Chem. Pharm. Bull.* **2021**, *69*, 1170−1178.

https://doi.org/10.1021/acscatal.4c00932
ACS Catal. 2024, 14, 7381−7388